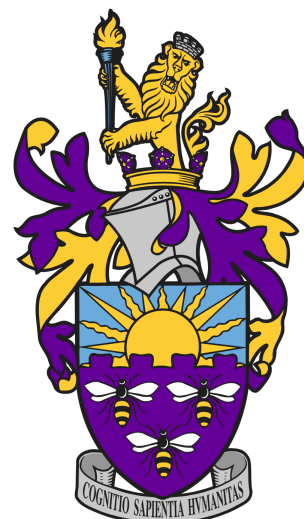# Bard School
Computing Lab

Cosmic Microwave Background

Boris Bolliet

Jodrell Bank Centre for Astrophysics
The University of Manchester

Day 3:

- Intro + questions

- New parameters inside CLASS

- MCMC with Montepython

Planck 2018 paper

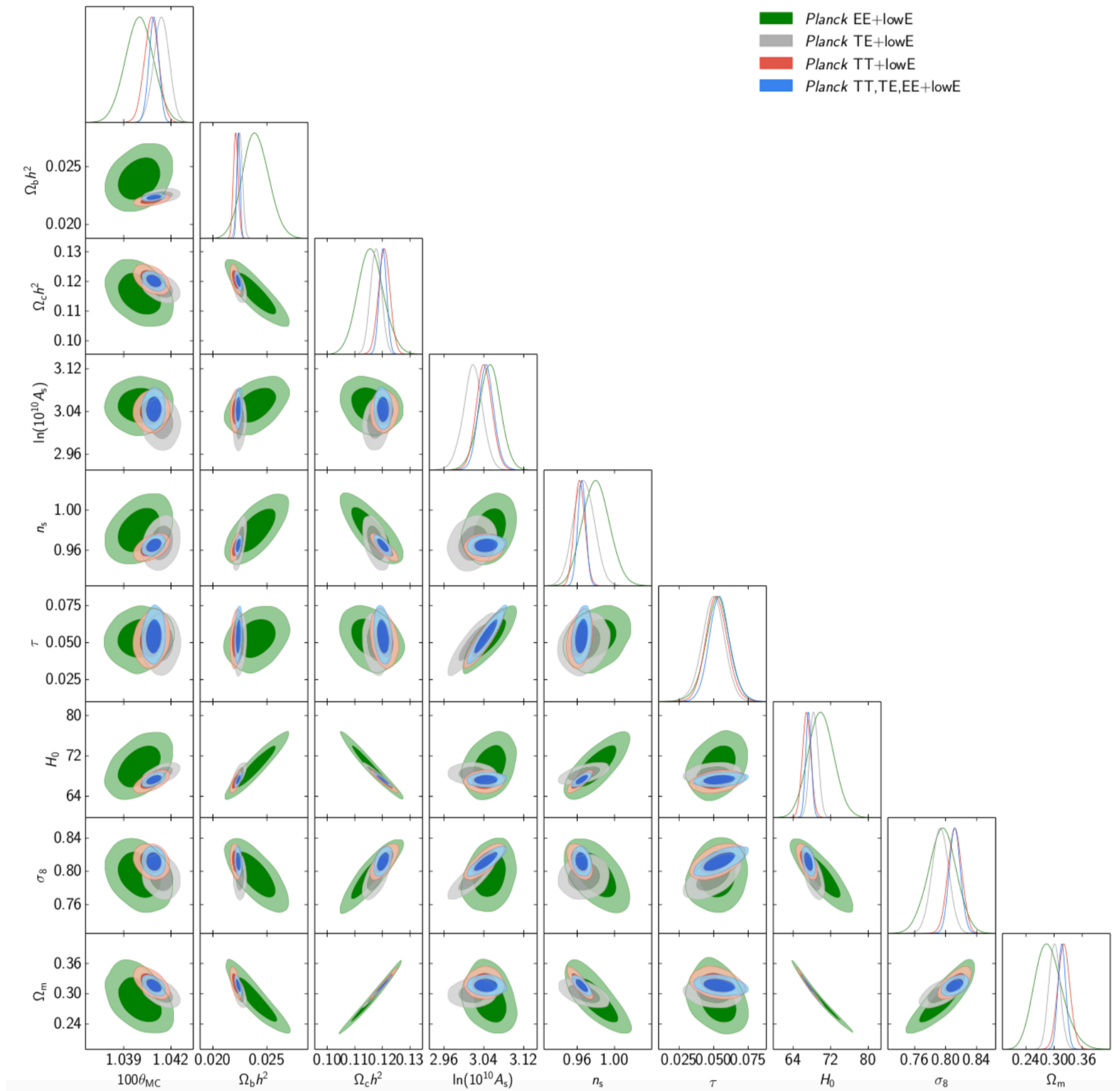| Parameter	Definition
$\omega_b \equiv \Omega_b\,h^2$	Baryon density today
$\omega_c \equiv \Omega_c\,h^2$	Cold dark matter density today
θ_{MC}	Approximation to the angular size of sound horizon at last scattering
τ	Optical depth to reionization
N_{eff}	Effective number of neutrino species
Σm_ν	Sum of neutrino masses
Ω_K	Spatial curvature parameter
w_0	Dark energy equation of state parameter
A_s	Scalar power spectrum amplitude
n_s	Scalar spectral index
$dn_s/d\ln k$	Running of scalar spectral index
$d^2n_s/d\ln k^2$	Running of running of scalar spectral index
r	Tensor-to-scalar power ratio
n_t	Tensor spectral index
$\epsilon_1 = -\dot{H}/H^2$	First Hubble slow-roll parameter
$\epsilon_{n+1} = \dot{\epsilon}_n/(H\epsilon_n)$	$(n+1)$st Hubble slow-roll parameter $(n \geq 1)$
$\epsilon_V = M_{pl}^2 V_\phi^2/(2V^2)$	First potential slow-roll parameter, where $_\phi \equiv d/d\phi$
$\eta_V = M_{pl}^2 V_{\phi\phi}/V$	Second potential slow-roll parameter
$\xi_V^2 = M_{pl}^4 V_\phi V_{\phi\phi\phi}/V^2$	Third potential slow-roll parameter
$\varpi_V^3 = M_{pl}^6 V_\phi^2 V_{\phi\phi\phi\phi}/V^3$	Fourth potential slow-roll parameter

Optical depth

3.1. Results for the scalar spectral index

Planck temperature data in combination with the EE measurement at low multipoles determine the scalar spectral tilt in the ΛCDM model as

$$n_{\mathrm{s}} = 0.9626 \pm 0.0057 \quad (68\,\% \text{ CL, } \textit{Planck} \text{ TT+lowE}) . \qquad (6)$$

This result for n_{s} is compatible with the *Planck* 2015 68 % CL value $n_{\mathrm{s}} = 0.9655 \pm 0.0062$ for *Planck* TT+lowP (PCP15). The slightly lower value for n_{s} is mainly driven by a corresponding shift in the average optical depth τ, now determined as

$$\tau = 0.052 \pm 0.008 \quad (68\,\% \text{ CL, } \textit{Planck} \text{ TT+lowE}) , \qquad (7)$$

Legend:
- *Planck* EE+lowE
- *Planck* TE+lowE
- *Planck* TT+lowE
- *Planck* TT,TE,EE+lowE

Boris Bolliet, JBCA Manchester - Bard College, 10-15 June 2019

Energy scale of inflation

$$V_* = \frac{3\pi^2 A_{\mathrm{s}}}{2} \, r \, M_{\mathrm{Pl}}^4 < (1.7 \times 10^{16} \text{ GeV})^4 \quad (95\,\% \text{ CL}) . \qquad (32)$$

Equivalently, this last result implies an upper bound on the Hubble parameter during inflation of

$$\frac{H_*}{M_{\mathrm{Pl}}} < 2.7 \times 10^{-5} \quad (95\,\% \text{ CL}) . \qquad (33)$$

Duration of inflation

$$N_* \simeq 67 - \ln\left(\frac{k_*}{a_0 H_0}\right) + \frac{1}{4} \ln\left(\frac{V_*^2}{M_{\mathrm{pl}}^4 \rho_{\mathrm{end}}}\right)$$

$$+ \frac{1 - 3w_{\mathrm{int}}}{12(1 + w_{\mathrm{int}})} \ln\left(\frac{\rho_{\mathrm{th}}}{\rho_{\mathrm{end}}}\right) - \frac{1}{12} \ln(g_{\mathrm{th}})$$

– The inflationary predictions (Mukhanov & Chibisov 1981; Starobinsky 1983) originally computed for the R^2 model (Starobinsky 1980) to lowest order,

$$n_s - 1 \simeq -\frac{2}{N}, \quad r \simeq \frac{12}{N^2}, \tag{48}$$

are in good agreement with *Planck* 2018 data, confirming the previous 2013 and 2015 results. The 95 % CL allowed range $49 < N_* < 58$ is compatible with the R^2 basic predictions $N_* = 54$, corresponding to $T_{\text{reh}} \sim 10^9\,\text{GeV}$ (Bezrukov & Gorbunov 2012). A higher reheating temperature $T_{\text{reh}} \sim 10^{13}\,\text{GeV}$, as predicted in Higgs inflation (Bezrukov & Shaposhnikov 2008), is also compatible with the *Planck* data.

– Monomial potentials (Linde 1983) $V(\phi) = \lambda M_{\text{Pl}}^4 (\phi/M_{\text{Pl}})^p$ with $p \geq 2$ are strongly disfavoured with respect to the R^2 model. For these values the Bayesian evidence is worse than in 2015 because of the smaller level of tensor modes allowed by BK14. Models with $p = 1$ or $p = 2/3$ (Silverstein & Westphal 2008; McAllister et al. 2010, 2014) are more compatible with the data.
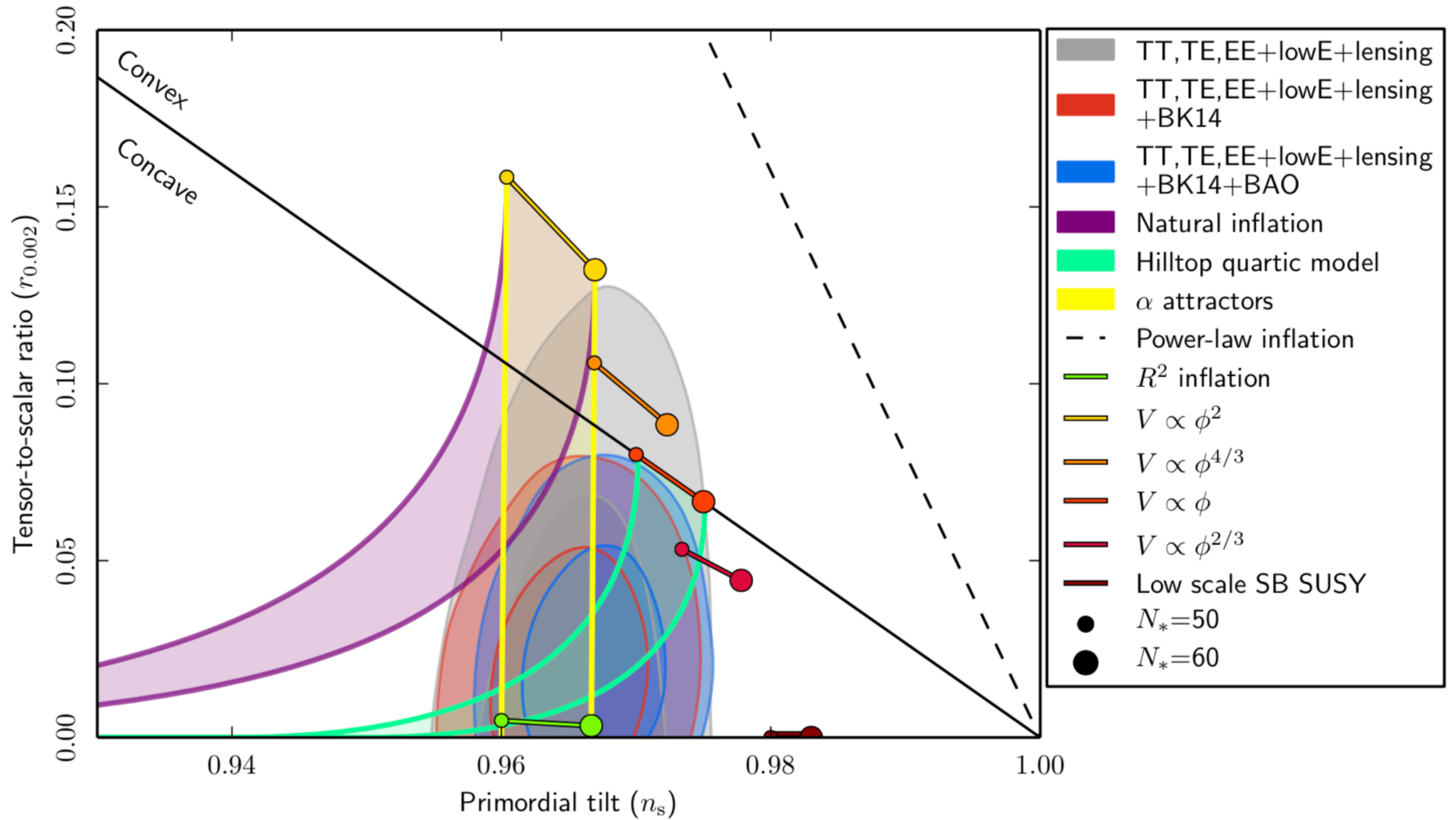
Boris Bolliet, JBCA Manchester - Bard College, 10-15 June 2019

Fig. 8. Marginalized joint 68 % and 95 % CL regions for n_s and r at $k = 0.002 \, \mathrm{Mpc}^{-1}$ from *Planck* alone and in combination with BK14 or BK14 plus BAO data, compared to the theoretical predictions of selected inflationary models. Note that the marginalized joint 68 % and 95 % CL regions assume $dn_s/d \ln k = 0$.
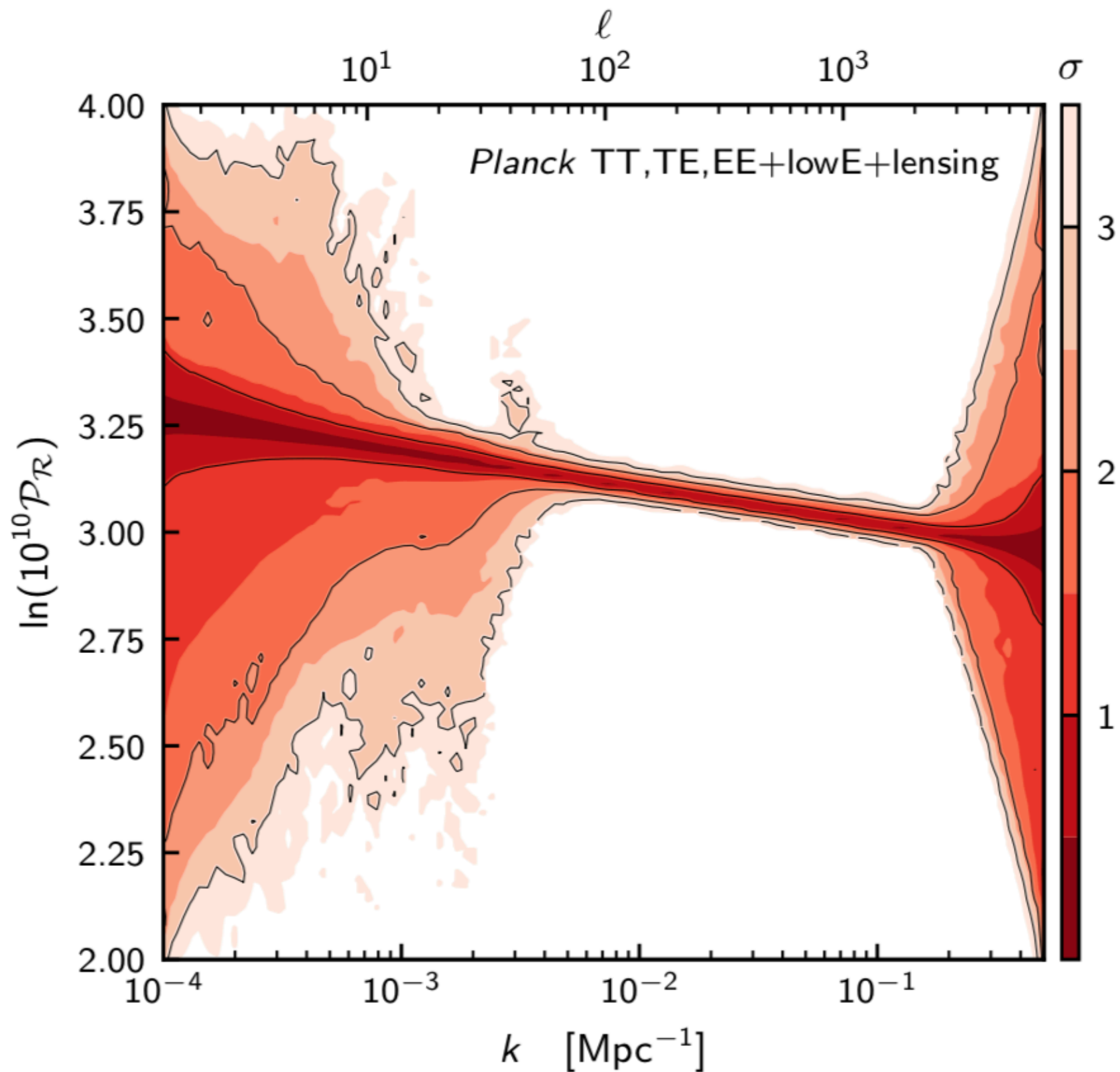
Fig. 20. Free-form Bayesian reconstruction of the primordial power spectrum (Sect. 6.2.1) using *Planck* TT,TE,EE+lowE+lensing. *Top-right:* Evidence values for each N-knot reconstruction. The evidence is maximal for the $N = 2$ and $N = 3$ knot cases, and semi-competitive for the remaining higher knots. Marginalizing over the number of knots produces a predictive posterior plot, shown in the top-left panel. Here we see generic features, with the limit of resolution of *Planck* at $\ell \simeq 2400$ and cosmic variance at low ℓ. *Bottom-left:* Same as top-left, but using the additional BK14 data and allowing r to vary. *Bottom-right:* Kullback-Leibler divergence conditional on k, marginalized over the number of knots, showing the increase in compression of the primordial power spectrum over several past CMB missions. The difference in constraining power between *Planck* 2013 and 2015 is driven entirely by the shift in the τ constraint.
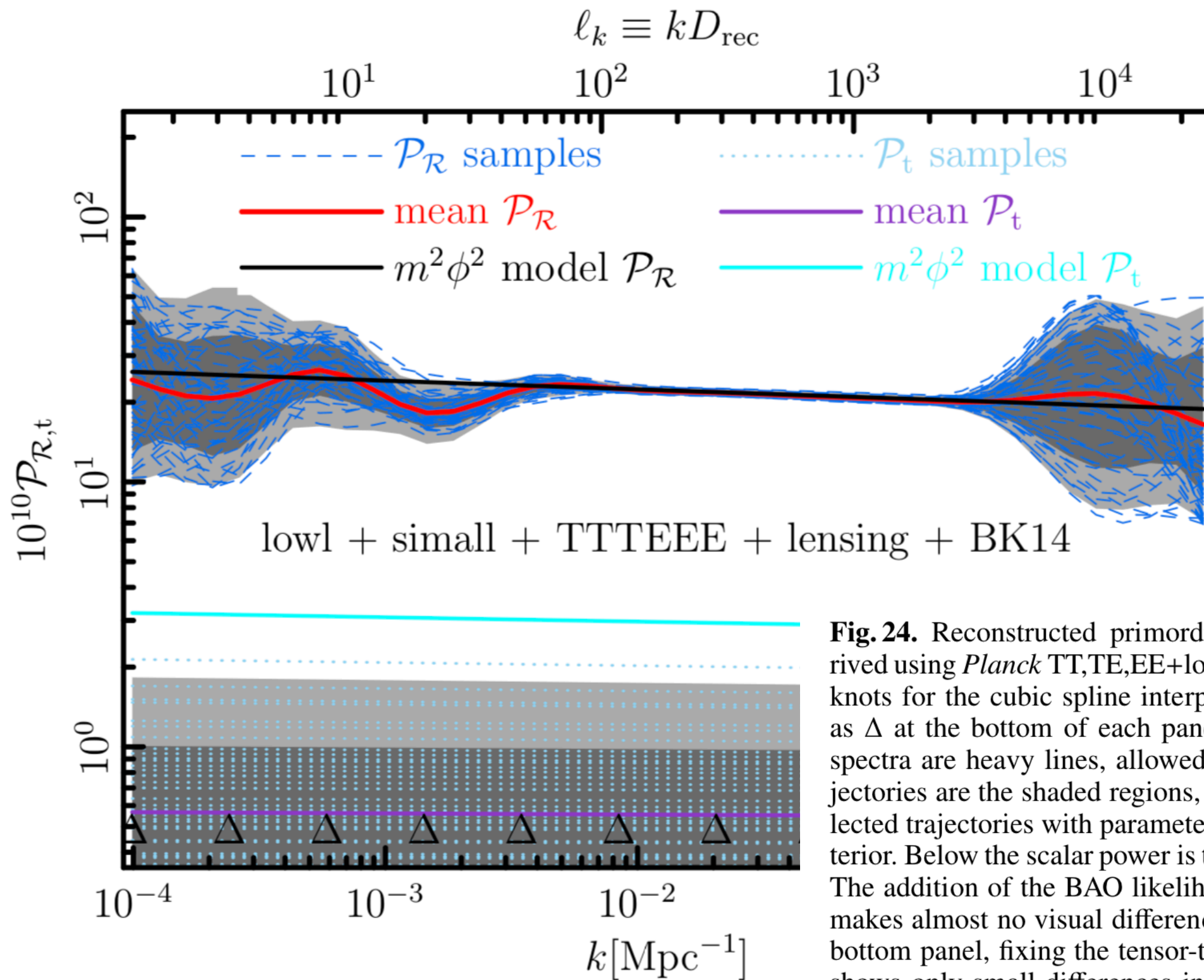
Fig. 24. Reconstructed primordial scalar power spectrum derived using *Planck* TT,TE,EE+lowE+lensing+BK14 data and 12 knots for the cubic spline interpolation (with positions marked as Δ at the bottom of each panel). Mean (ensemble-averaged) spectra are heavy lines, allowed $\pm 1\sigma$ and $\pm 2\sigma$ regions for trajectories are the shaded regions, and the dashed lines denote selected trajectories with parameters sampled within the $\pm 1\sigma$ posterior. Below the scalar power is the tensor power reconstruction. The addition of the BAO likelihood shown in the middle panel makes almost no visual difference to the reconstructions. In the bottom panel, fixing the tensor-to-scalar ratio to $r = 0.001$ also shows only small differences in reconstruction. Knot positions in k roughly translate to multipoles through $kD_{\rm rec}$, where $D_{\rm rec}$ is the comoving distance to recombination.

# 7. Search for primordial features in the *Planck* power spectrum

The "bottom-up" power spectrum reconstruction methods of the previous section are an excellent way to search for coarse features in the spectrum, but lack the resolution to detect the higher-frequency features generically predicted by various physical mechanisms [see, e.g., Chluba et al. (2015) for a review]. It is therefore useful to complement power spectrum reconstruction with a "top-down" approach by fitting specific feature models to the data. In this section we will analyse a representative range of power spectrum templates which parameterize features in terms of a handful of new parameters.

7. *Is there evidence for features in the primordial power spectrum?*

We explored several classes of theoretically motivated parametric models with strong departures from a power law for the primordial power spectra and tested their predictions using combinations of *Planck* temperature and polarization power spectra. We also carried out an analysis using bispectrum data as well. No statistically significant evidence for features was found.
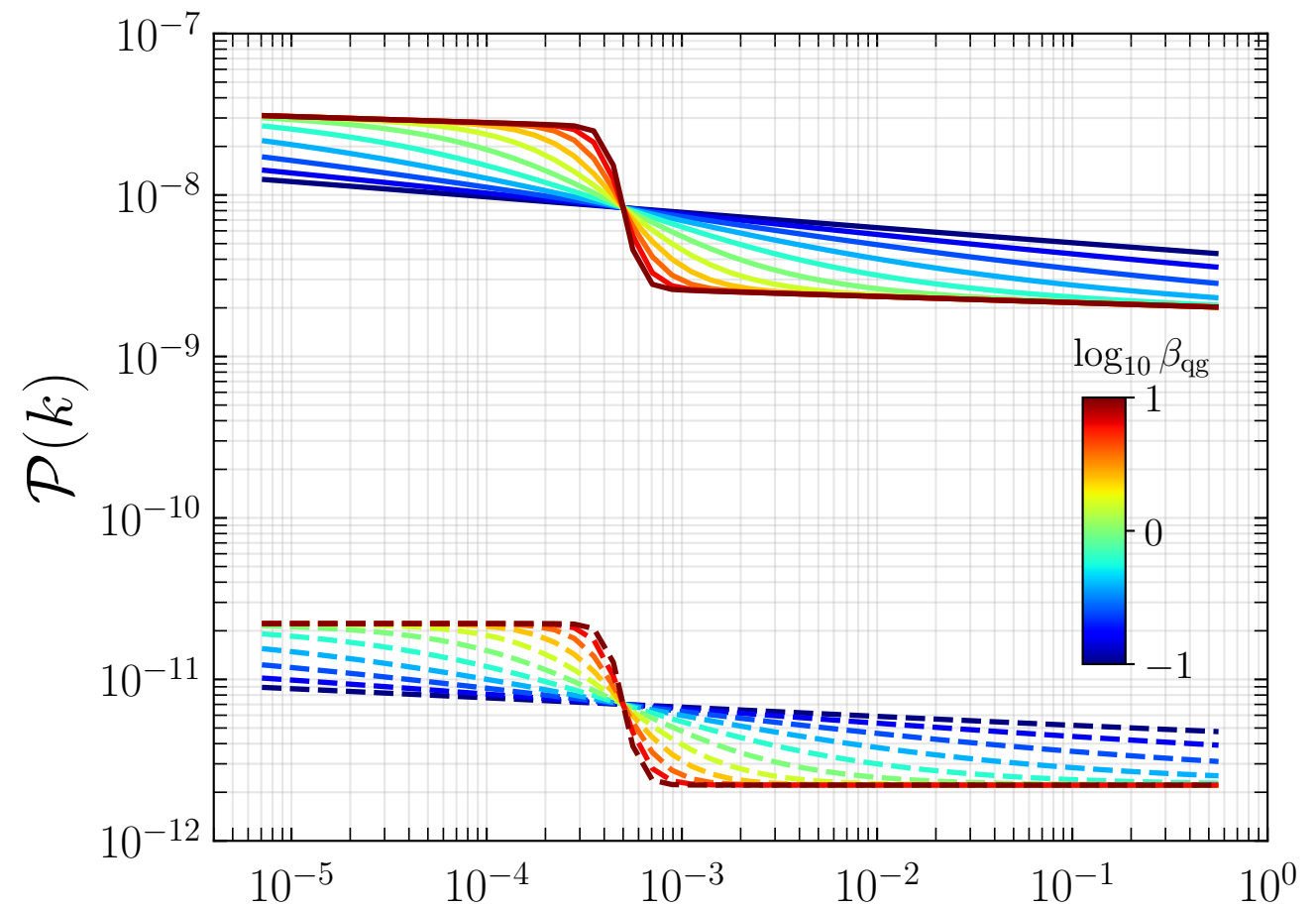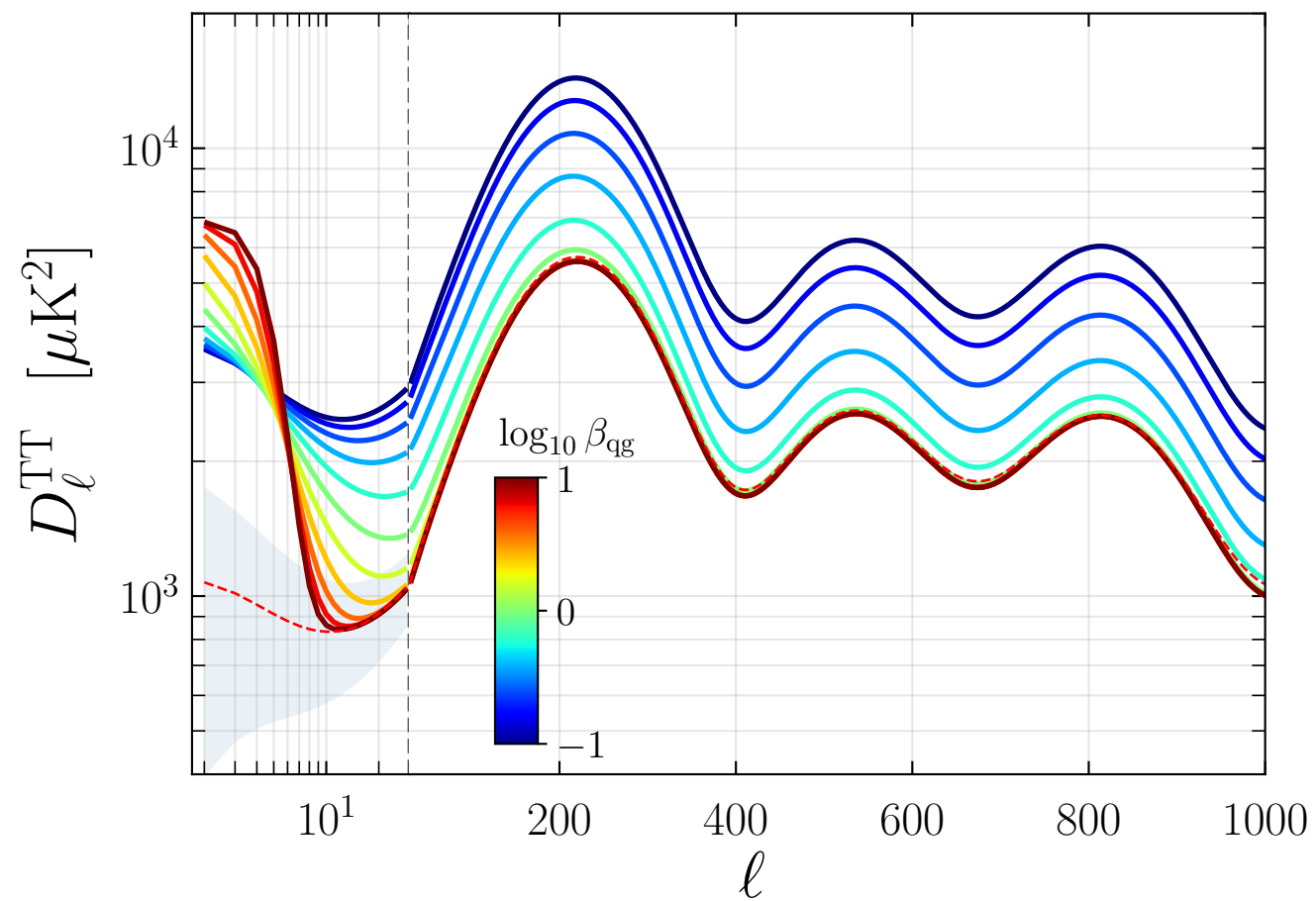
Boris Bolliet, JBCA Manchester - Bard College, 10-15 June 2019

Phenomenological parameterisation of primordial power spectrum

$$\frac{\mathcal{P}_{\mathrm{QG}}}{\mathcal{P}_{\mathrm{SR}}} = \exp\left(\frac{\ln\alpha}{1 + \left(\frac{k}{k_{\mathrm{QG}}}\right)^{\beta}}\right)$$
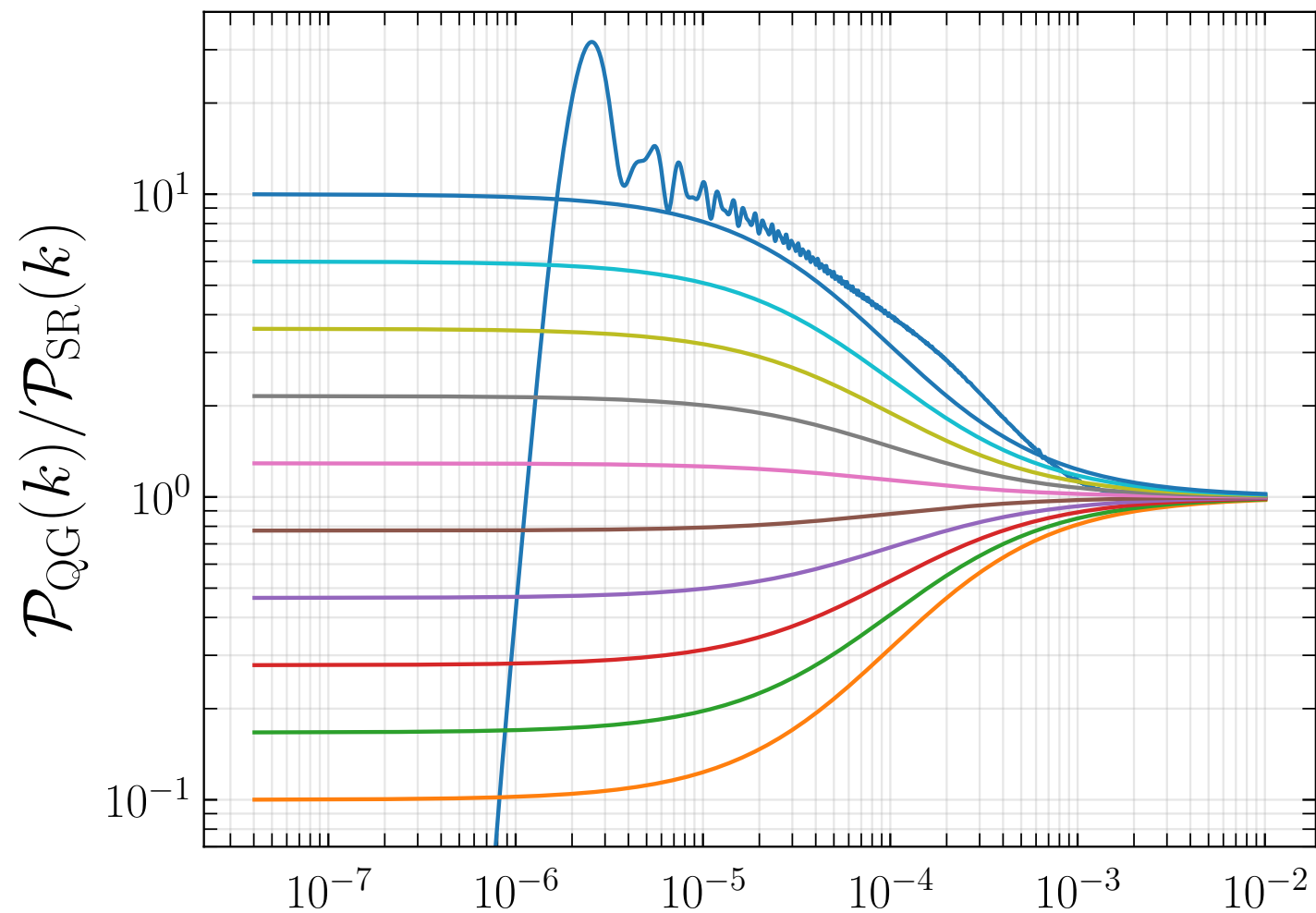
Varying alpha

```
alpha_qg = 1.e1
beta_qg =10.0
k_qg_over_k_pivot = 1.e-2
```

$$\frac{\mathcal{P}_{\mathrm{QG}}}{\mathcal{P}_{\mathrm{SR}}} = \exp\left(\frac{\ln\alpha}{1 + \left(\frac{k}{k_{\mathrm{QG}}}\right)^{\beta}}\right)$$

Boris Bolliet, JBCA Manchester - Bard College, 10-15 June 2019